



# Measurement of the Sunyaev-Zel'dovich effect with the SRT

M. Gervasi<sup>1</sup>, G. Boella<sup>1</sup>, G. Sironi<sup>1</sup>, A. Tartari<sup>1</sup>, M. Zannoni<sup>1</sup>, and V. Natale<sup>2</sup>

<sup>1</sup> Università di Milano Bicocca, Dip. di Fisica, Piazza della Scienza 3, I-20126 Milano

<sup>2</sup> INAF - Istituto di Radioastronomia, Sez. di Firenze, Largo E. Fermi 5, I-50125 Firenze

## Abstract.

The Sunyaev-Zel'dovich effect is a powerful probe useful to investigate both the properties of galaxy clusters and cosmological parameters. We are developing low-noise SIS mixer-based receivers for continuum observations at 90 GHz. By using these receivers at the SRT we can investigate galaxy clusters at high redshift, where the typical core *radii* are comparable to the angular resolution of the telescope at 100 GHz. These sources are largely unexplored but their interest will be increasing in the near future due to X-ray observations from satellites.

## 1. Introduction

The Sunyaev-Zel'dovich effect (SZe) is a powerful probe to investigate the properties of the intra-cluster medium (ICM) and the physical processes occurring inside the galaxy clusters. Apart from its astrophysical relevance, SZe can provide an important experimental mine where information about cosmological parameters can be extracted. Among these we mention the Hubble constant  $H_0$ , the cluster gas-mass fraction and  $\sigma_8$  (Borgani et al. 2001). Moreover, we recall that SZe is a promising tool to trace the evolution of the Cosmic Microwave Background temperature with  $z$  and to detect large-scale peculiar motions. For a thorough review on the cosmological impact of the SZe see Carlstrom et al. (2002), Birkinshaw (1999), and Rephaeli (1995). The thermal SZe arises from the interaction of the hot ionized intra-cluster medium with the photons of the CMB by means of the inverse Compton scattering (Zel'dovich & Sunyaev 1969; Wright 1979). CMB photons

gain energy after this process and a fraction of them moves towards higher frequency. The observed spectrum results distorted: a depletion is present at frequencies lower than the cross-over  $x_0$ , where the effect is null, while an enhancement can be observed at higher frequencies (this is clearly represented in Fig. 1).

The cross-over occurs at a frequency  $x_0 = h\nu_0/k_B T_{cmb} \approx 3.830$ , which means  $\nu_0 \approx 218$  GHz. The amount of the effect depends on the Comptonization parameter  $y$  defined as

$$y = \int n_e \frac{k_B T_e}{m_e c^2} \sigma_T d\ell, \quad (1)$$

which is clearly related to the optical depth  $\tau_e = \int n_e \sigma_T d\ell$ . Here  $T_e$  and  $n_e$  are the temperature and density of the electron plasma;  $\sigma_T$  is the cross section of the Thompson scattering. The brightness temperature variation is

$$\frac{\Delta T_{SZe}}{T_{cmb}} = y \left( x \frac{e^x + 1}{e^x - 1} - 4 \right) (1 + \delta_{SZe}), \quad (2)$$

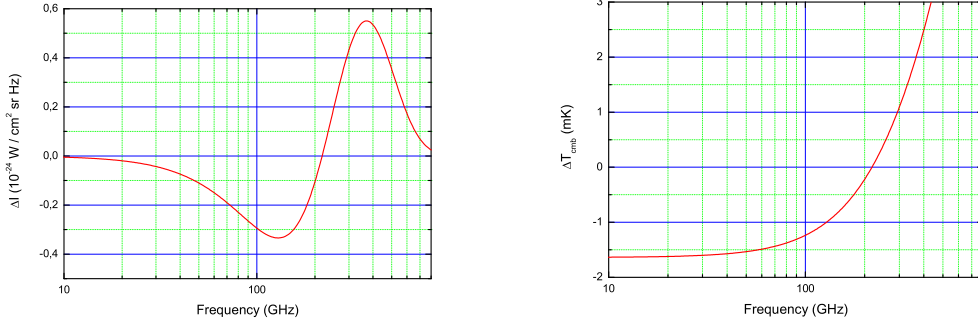


**Fig. 1.** The thermal SZe for the case  $y = 1 \times 10^{-4}$ . *Left panel:* brightness variation with respect to the undistorted spectrum. *Right panel:* black-body temperature variation with respect to the undistorted one.

where  $\delta_{SZe}$  is the relativistic correction. The corresponding intensity variation is

$$\frac{\Delta I_{SZe}}{I_{cmb}} = y \frac{x^4 e^x}{(e^x - 1)^2} \left( x \frac{e^x + 1}{e^x - 1} - 4 \right) (1 + \delta_{SZe}). \quad (3)$$

The temperature of the cluster gas is increasing with the cluster total mass, and its typical values fall in the range  $k_B T_e \sim 5 - 15$  keV. At these temperatures the electron velocities approach the relativistic regime and the corrections described are effective.

There is another effect which is not negligible: the kinematic Sunyaev-Zel'dovich (SZk). It is due to the peculiar motion of the cluster with respect to the Hubble flow (i.e. the CMB rest frame) and is proportional to the cluster velocity  $v_p$  times the optical depth of the plasma, so that the temperature variation is

$$\frac{\Delta T_{SZk}}{T_{cmb}} = -\tau_e \frac{v_p}{c}. \quad (4)$$

The amount of this effect is of the order of  $\Delta T_{SZk} \sim 10 \mu\text{K}$ . This value must be compared with the thermal SZe, which is  $\Delta T_{SZe} \sim \text{few } 100 \mu\text{K}$ .

A necessary remark on these two distinct effects is that while the thermal SZe has a spectral signature which is different from the primary anisotropies of the CMB, SZk has the same frequency dependence and is potentially indistinguishable from them.

## 2. Clusters at high redshift

Clusters of galaxies are the greatest collapsed structures ever observed, and they provide unique probes to understand the physics of the early Universe. The processes underlying the formation of these objects are still matter of debate, even if it seems likely that clusters are formed by the infall of baryonic matter into the potential wells created by dark matter (DM) over-densities. In turn, the distribution of DM along large-scale filaments and the depth of potential wells trace the evolution of primordial density fluctuations primed during the inflationary era. The X-ray emission from the ICM (mainly due to thermal bremsstrahlung), and the thermal SZe, sensitive respectively to  $n_e^2$  and  $n_e$  ( $n_e$  is the electron density in the intra-cluster plasma), are two of the most relevant physical processes by which we can improve our knowledge of the formation and evolution of clusters of galaxies.

This aim can be achieved studying the scaling laws characterizing the ICM (e.g. the luminosity-temperature relation in X-rays,  $L_x - T_x$ ) and their redshift dependence, as shown in Tozzi & Norman (2001). Scaling relations can also be built combining SZe and X-ray observables, since the number of clusters observed by millimeter-wave observatories and X-ray satellites is rapidly increasing, and studies in which these spectral regions have been jointly exploited have already been published (e.g. Pointecouteau et al. 2002). McCarthy et al. (2003a,b) have also pointed out the impor-

**Table 1.**

Name	$\alpha$	$\delta$	redshift	$T_e$ (keV)	$\theta_c$ (arcsec)
RX J2228+2037 <sup>1</sup>	22 <sup>h</sup> 28 <sup>m</sup> 33 <sup>s</sup>	20°37'12''	0.42	10.4 ± 1.8	20.3 ± 3.1
RX J1120.1+4318 <sup>2</sup>	11 <sup>h</sup> 20 <sup>m</sup> 07 <sup>s</sup>	43°18'05''	0.60	5.6 <sup>+0.25</sup> <sub>-0.3</sub>	27.4 ± 1.2
RX J1334.3+5030 <sup>2</sup>	13 <sup>h</sup> 34 <sup>m</sup> 20 <sup>s</sup>	50°30'54''	0.62	5.20 <sup>+0.26</sup> <sub>-0.28</sub>	20 ± 1
CIJ1324+3011 <sup>3</sup>	13 <sup>h</sup> 24 <sup>m</sup> 50 <sup>s</sup>	30°11'25''	0.76	2.88 <sup>+0.71</sup> <sub>-0.49</sub>	7.4 ± 1.4
CIJ1226.9+3332 <sup>4</sup>	12 <sup>h</sup> 26 <sup>m</sup> 58 <sup>s</sup>	33°32'45''	0.89	11.5 <sup>+1.1</sup> <sub>-0.9</sub>	14.5 <sup>+0.2</sup> <sub>-0.8</sub>
CIJ1604+4304 <sup>3</sup>	16 <sup>h</sup> 04 <sup>m</sup> 19.5 <sup>s</sup>	43°04'34''	0.90	2.51 <sup>+1.05</sup> <sub>-0.69</sub>	7.7 ± 0.3
RDCS 0849+4452 <sup>5</sup>	08 <sup>h</sup> 48 <sup>m</sup> 56 <sup>s</sup>	44°52'00''	1.26	4.7 ± 1	~ 6

1: Pointecouteau et al. (2002); 2: Lumb et al. (2004); 3: Lubin et al. (2004);

4: Maughan et al. (2004); 5: Rosati et al. (1999).

$T_e$  is the electron temperature of the plasma;  $\theta_c$  is the core radius.

tance of scaling relations derived by SZe alone for the study of the thermodynamical properties of the ICM. Moreover, unlike X-ray emission, this effect is not subject to cosmological dimming, allowing deeper cluster surveys and possibly the detection of objects which couldn't be otherwise observed. In fact wide surveys of the SZe are planned in the near future both from space (e.g. *Planck*) and from ground observatories (mainly *SPT*, *APEX* and *ACT*).

The large aperture of the SRT and its surface accuracy (which allows observations up to 100 GHz) make this telescope a prominent candidate for the detection of clusters of galaxies at cosmological distances by means of the thermal SZe<sup>1</sup>. In fact the angular resolution at 100 GHz ( $\sim 11''$ ), in spite of the reduction of the aperture efficiency (it falls at 0.35), is enough to obtain a beam comparable to the size of the core *radii* of some representative clusters listed in Table 1. These clusters have been already detected by *XMM*, *ROSAT* and *CHANDRA* and fall in sky regions which can be covered by the SRT during the winter period. The parameters quoted in Table 1 have been extracted by the authors fitting the observational data to isothermal  $\beta$ -models and assuming the usual flat spacetime geometry with  $H_0 = 70 \text{ km s}^{-1}/\text{Mpc}$ .

<sup>1</sup> We underline that since a frequency band around the crossover is not available, it is impossible to single out the kinematic SZe.

### 3. Receivers and observing strategy

The natural observing technique for the detection of the SZe is the beam switching between on-source and off-source positions. The angular extent of the modulation has to guarantee that the beam in the off-position is completely outside the cluster. Practically, if we refer to the specific case of CIJ1226.9+3332 (Maughan et al. 2004), where the X-ray emission has been detected 100'' away from the X-ray centroid, and if we remember that the SZ profile is wider than the X-ray diameter of the source, then we conclude that the beam throw has to be at least 2'.

What kind of signals contribute to the differential output apart from the SZ decrement? If the beam switching takes place between sky regions separated by an angle  $\Delta\theta$ , the signals which are statistically anisotropic on this angular scale won't be cut on average. For example the CMB primary anisotropies corresponding to the multipole index  $\ell \sim 1/\Delta\theta$  will survive, and the same is true for the galactic foregrounds<sup>2</sup>. On the contrary the isotropic foregrounds will be completely removed. In principle also the dust surviving into the hot ICM could contribute to the amplitude of the differential signal, but its contribution could be important at frequencies beyond  $\sim 300$  GHz.

<sup>2</sup> Apart from diffuse foregrounds, another source of possible contamination is represented by point sources.

### 94-GHz Mixer Mount

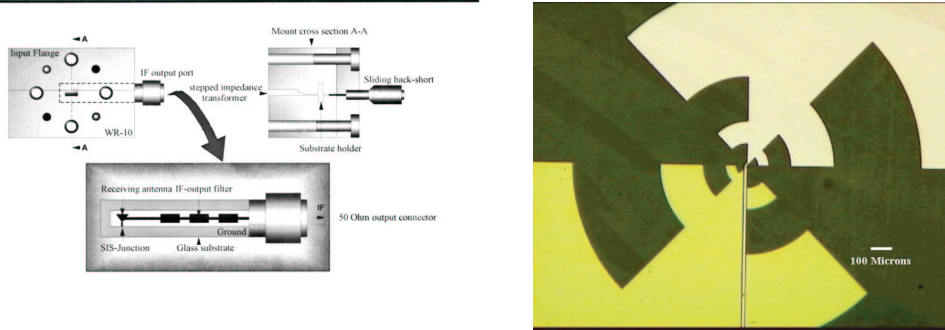


**Fig. 2.** *Left panel:* the waveguide mounting of the 94 GHz SIS mixer. *Right panel:* the log-periodic antenna, needed to couple the electromagnetic wave to the SIS junction, fixed to the rear of the quartz hyperhemispherical lens.

Also the atmosphere could contribute through spatially correlated fluctuations, and they represent by far the most serious obstacle for an observational campaign at 100 GHz aimed at cosmological targets. Therefore a preliminary and accurate site testing is mandatory.

We propose to develop a multi-pixel radiometer based on SIS mixers, optimized for SZE observations, as focal plane instrumentation for SRT in the 90-110 GHz frequency band. At present we are working in collaboration with the I.E.N. "Galileo Ferraris" in Torino, where both waveguide-mounted mixers and open-structure mixers are under study<sup>3</sup> (Fig. 2), while a millimeter-wave testing facility has already been prepared at the Physics Department of the University of Milano Bicocca. Let's give a short glance at the expected performance of a SIS mixer receiver. At 100 GHz a typical front-end chain constituted by feed horn, SIS mixer and LNA, has a noise temperature lower than 100 K, so when the receiver is looking at the cold sky, the system temperature is expected to be less than 150 K, corresponding to an instantaneous sensitivity of  $\sim 5 \text{ mK}/\sqrt{\text{Hz}}$  (an integration IF bandwidth  $\Delta\nu = 1.2 \text{ GHz}$  is assumed for a DSB configuration, while the ef-

iciency is that of a Dicke receiver). In a worst-case situation in which the sensitivity is degraded to  $7 \div 8 \text{ mK}/\sqrt{\text{Hz}}$ , a  $\Delta T = 60 \mu\text{K}$  can be detected at  $1\sigma$  level in 5 hours, while 45 hours are required to reach  $20 \mu\text{K}$ . Anyway we have to deal carefully with these quantities, since they are obtained from the *radiometer equation*, which has a purely statistical meaning. In the real world instabilities ( $1/f$  gain fluctuations) could arise in the receiver for long integration times, even if they can be controlled by modulation-demodulation techniques (Wollack 1995). The atmosphere itself could be a source of low-frequency drifts of the signal, since its noise is partially time-correlated. Concerning the issue of stability, the cooling mechanism is important too. As shown by Kooi et al. (2000), who studied the onset of instabilities by means of Allan plots, the knee frequency<sup>4</sup> changes appreciably if we cool the same front-end in a standard liquid helium dewar, or by a pulse tube cooler, or by a mechanical cryocooler. From this point of view the pulse tube cooler is a good compromise, since its Allan time is greater than that of a cryocooler, while it is more practical than a LHe dewar (especially for a long observational campaign). The drawback is that the cold head has to be held at less than  $30^\circ$  from the vertical po-

<sup>3</sup> Multi-pixel SIS receivers are currently developed using both guided and open structures (Barychev 2005)

<sup>4</sup> The critical frequency where *colored* noise overcomes the white noise floor.

sition in order to prevent efficiency losses, so that the optical configuration should take into account this limitation.

A last issue which we would like to face in conclusion is the improvement of the detection of clusters' physical parameters, such as  $y$ , by increasing the number of channels. In order to obtain indicative trends of the uncertainty on the Comptonization parameter for clusters whose  $T_e$  is already known, we have used the SASZ Fortran code written by S. Hansen. We have found that the situation doesn't change appreciably if we have two channels in the same frequency band (say 90 GHz and 100 GHz) or a single channel (at 90 GHz) operating with the same sensitivity. In both cases, for a relaxed cluster like CIJ1226.9+3332, we have obtained  $\log y = -4.2 \pm 0.1$  after 5 hours of integration (assuming the typical efficiency of a Dicke receiver), corresponding to a relative uncertainty between 21% and 26%. Consequently, the important practical consideration is that in the frequency band 90-110 GHz we can pump the two (or more) SIS mixers with the same Local Oscillator wave. The quality of the detection improves considerably if a second receiver in a different frequency band is available. Particularly important for the study of the SZ effect is the  $K_a$ -band around 30 GHz, where low noise amplifiers are commonly available. In fact with a third channel operating at this frequency, in the same integration time (5 hours), we have  $\log y = -4.21 \pm 0.06$ , and a relative uncertainty in  $y$  between 13% and 15%. This is exactly what we could expect *a priori*, since we have extended the frequency leverage, imposing a stronger constraint on the available region in the parameter space<sup>5</sup>. Moreover, if also a receiver at 30 GHz could be operated simultaneously with the multi-pixel SIS radiometer, we could have a better control on foregrounds. Without the third frequency in the  $K_a$ -band, but increasing the integration time to 45 hours, the relative uncertainty in  $y$

falls to 5%. Assuming again that we have two channels at 90 GHz and 100 GHz, but with a wider integration bandwidth, say 4 GHz<sup>6</sup>, in 45 hours we obtain again  $\log y = -4.20 \pm 0.02$  (corresponding to the 5% uncertainty), but without any prior knowledge coming from X-rays detections.

*Acknowledgements.* We are grateful to Steen Hansen for bringing his SASZ code to our attention.

## References

- Barychev, A. 2005, PhD Thesis, Technische Universiteit Delft (NL)
- Birkinshaw M. 1999, Phys. Rep., 310, 97
- Borgani, S., Rosati, P., Tozzi, et al. 2001, ApJ, 561, 13
- Carlstrom, E.C., Holder, G.P., & Reese, E.D. 2002, ARA&A, 40, 643
- Kooi, J.W., Chattopadhyay, G., Thielman, M., Phillips, T.G., & Schieder, R. 2000, Int. J. MM and IR waves, 21, 689
- Lubin, L.M., Mulchaey, J.S., & Postman, M. 2004, ApJ, 601, L9
- Lumb, D.H., Bartlett, J.G., Romer, A.K., et al. 2004, A&A, 420, 853
- Maughan, B.J., Jones, L.R., Ebeling, H., & Scharf, C. 2004, MNRAS, 351, 1193
- McCarthy, I.G., Babul, A., Holder, G.P., & Balogh, M.L. 2003a, ApJ, 591, 515
- McCarthy, I.G., Holder, G.P., Babul, A., & Balogh, M.L. 2003b, ApJ, 591, 526
- Pointecouteau, E., Hattori, M., Neumann, D., et al. 2002, A&A, 387, 56
- Rephaeli, Y. 1995, ARA&A, 33, 541
- Rosati, P., Stanford, S.A., Eisenhardt, P.R., et al. 1999, AJ, 118, 76
- Tozzi, P., & Norman, C. 2001, ApJ, 546, 63
- Wollack, E.J. 1995, Rev. Sci. Instrum., 66, 4305
- Wright, E.L. 1979, ApJ, 232, 348
- Zel'dovich, Ya.B. & Sunyaev, R.A. 1969, Ap&SS, 4, 301

<sup>5</sup> Neglecting the peculiar motions of the cluster, the parameters fixed by the likelihood analysis are  $T_e$  and  $y$ , since  $\chi^2(y, v_p, T_e)$ .

<sup>6</sup> The ALMA band 3 receiver is currently designed to operate with a 4-GHz signal sideband.